Spectral & Temporal Studies of Multiply Scattered Ultra-Broadband Light

A Thesis

submitted to

Indian Institute of Science Education and Research Pune
in partial fulfillment of the requirements for the
BS-MS Dual Degree Programme

by

Sharvari Zilpelwar

Indian Institute of Science Education and Research Pune
Dr. Homi Bhabha Road,
Pashan, Pune 411008, INDIA.

April, 2018

Supervisor: Sushil Mujumdar

© Sharvari Zilpelwar   2018

Certificate

This is to certify that this dissertation entitled Spectral & Temporal Studies of Multiply Scattered Ultra-Broadband Light towards the partial fulfilment of the BS-MS dual degree programme at the Indian Institute of Science Education and Research, Pune represents study/work carried out by Sharvari Zilpelwar at Tata Institute of Fundamental Research under the supervision of Sushil Mujumdar, Assistant Professor, Department of Nuclear and Atomic Physics, during the academic year 2017-18.

Sushil Mujumdar

Committee:

Sushil Mujumdar

GV Pavan Kumar

This thesis is dedicated to my parents

Declaration

I hereby declare that the matter embodied in the report entitled Spectral & Temporal Studies of Multiply Scattered Ultra-Broadband Light are the results of the work carried out by me at the Department of Nuclear and Atomic Physics, Tata Institute of Fundamental Research, Mumbai, under the supervision of Sushil Mujumdar and the same has not been submitted elsewhere for any other degree.

Sharvari Zilpelwar

Acknowledgments

First and foremost, I wish to express my sincere gratitude to my supervisor, Prof. Sushil Mujumdar for providing me an opportunity to work on my Master's Thesis in his laboratory. His firm commitment and dedication in resolving my doubts and understanding the difficulties in conducting experiments has helped me throughout the course of my stay at TIFR, Mumbai. I sincerely thank Dr. Aditya Dharmadhikari and Dr. Jayashree Dharmadhikari for their valuable inputs and giving me hands-on experience of the femtosecond laser facility at TIFR and for other relevant scientific discussions.

I also take this opportunity to express a deep sense of gratitude to all my lab members of Nano Optics and Mesoscopic Optics Laboratory (NOMOL) who have been there to train me in terms of values and hands-on experience on nanosecond, picosecond laser, streak camera. Dr. Balasubrahmaniyam has helped me to tackle issues arising in experimentation and ways of improvising the setup along with discussion on diffusion, plasmonics and physics in general. Sreeman has been a great helping hand for solving all the issues in the laboratory to maintain the normal working standards of all instruments. My colleagues Ashwin, Sandip, Krishna, Rabisankar, Shweta, Randhir and Shabna have helped me in all scientific and in non-scientific way like lending me their laptops, assisting me to help me move the optics from lab to lab and their constant inputs. Last but not the least, I thank all my IISER Pune-TIFR friends for making my stay memorable.

x

Abstract

Mesoscopic light transport through disordered medium (randomly scattering medium) is an ubiquitous phenomenon. Understanding this transport phenomenon is of fundamental importance and helps to answer the unsolved questions about light transport in three-dimensional random systems. Here, we look at the spatial and temporal characteristics of a ultra-broadband and ultra-short coherent light pulse as it travels through a strongly scattering random medium. We launch supercontinuum pulse into the strongly scattering medium to measure the backscattered spectrum (using femtosecond laser) and transmitted spectrum measurements (using ytterbium doped fiber). We report out spectral profile in image plane at different concentration and in Fourier plane at different distances at a given concentration to isolate ballistic light from diffused light. The calculation of temporal profile of the transmitted light is carried out and decay parameters were identified for the system under study.

Contents

Chapter 1

Multiple Scattering of Light

1.1 Introduction

The beautiful strokes of colours seen at the sunrise and sunset and blue colour of the sky are the results of wavelength and size dependent scattering of light in the atmosphere. Many such phenomena like Tyndall effect or rare phenomena of the blue moon is the result of scattering.

Light transport through a multiply scattering media undergoes deviation from its path and travels for a longer time in the media. Depending on the input wavelength, size of the particle, system properties (size of the particle, refractive index, particle density), light can either be localized [1] or diffused. The field of light transport through inhomogeneous media has been well-studied and has applications in the domain of biomedical imaging [2], adaptive optics [3], solar cells [4].

Throughout this thesis, we are concerned about the diffusion of light through an inhomogeneous media. The purpose of the study is to understand the wavelength dependent diffusion profile and its effect on the ultra-broadband wavelength range. To study the diffusion profile, we look at the spectral profile in the forward and backward scattered direction as the diffusion profile at large time scales in both cases will be same [5] [6]. We have also carried out studies in Fourier plane to isolate ballistic and diffused light. The results of all these studies have been presented here which can further be helpful to make temporal profile
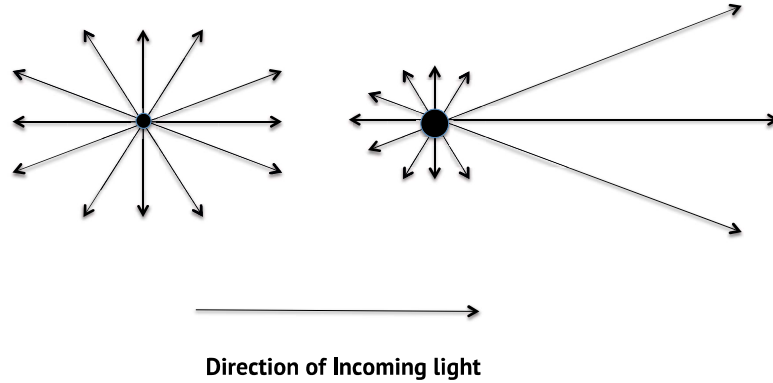
Direction of Incoming light

Figure 1.1: *The distribution of photons for spherical particles is isotropic (left) and anisotropic (right) which is dependent on the size of the particle and the incoming wavelength.*

measurements to estimate the decay coefficient of the ultra-broadband light.

1.2   Physics of Multiple Scattering

When an electromagnetic wave is incident on a single particle, the total energy in all directions will be the sum of the energies scattered from a virtual cross-sectional area defined as scattering cross-section (σ_s). If the particle is absorbing energy, the sum of absorption cross-section and scattering cross-section ($\sigma_e = \sigma_a + \sigma_s$) is the extinction cross-section. These cross-sections depend on the polarisation and angle of incidence of the electromagnetic wave. In the current study, we are considering only σ_s as we are choosing non-absorbing particles. Light scattering is dependent on size parameter (x) given by:

$$x = \frac{2\pi a}{\lambda}$$

where a is the particle size and λ is the incident wavelength.
For Rayleigh range, x $<<$ 1 i.e. particle size is smaller than wavelength. The electric field inside the particle will not have any spatial variation. Scattering is anisotropic even for spherical particles when particle size which is comparable to wavelength (fig.1.1).

For a single particle in Rayleigh regime, for a given incident intensity (I_0), the intensity

measured (I) at a distance (R) from the center at the scattering angle (θ) measured from the normal for a particular wavelength λ is given by [7] :

$$I = I_o \frac{8\pi^4 N \alpha^2}{\lambda^4 R^2} (\frac{n^2 - 1}{n^2 + 2})(1 + \cos^2 \theta) \qquad\qquad I \propto \frac{N}{\lambda^4} \qquad\qquad (1.1)$$

where n is the ratio of refractive index of the scatterer to the surrounding medium, N is the scatterer density and α is the polarizability. Thus, we would expect the intensity to drop proportional to the fourth power of the wavelength. If an ultra-broadband white light is incident on a multiply scattering media, the scattered intensity $(\cos \theta = 0)$ is higher for smaller wavelengths than for larger wavelengths.

When we expand our theory from single scattering to multiple scattering,it is very difficult to trace the path and phase information about the photon as it undergoes many collisions in the sample. This system can be approximated to be a random walk system where all the collisions are independent of each other. The most important parameter governing such system is the average distance between two successive collisions called as scattering mean free path.

$$l_s = \frac{1}{N\sigma_s} \qquad\qquad (1.2)$$

where N is the scatterer density and σ_s is the scattering cross-section. But the anisotropy of the system gives preference to one direction over other. We define a new length parameter called transport mean free path (l^*) taking the anisotropy parameter (g) into account.

$$l^* = \frac{l_s}{(1 - g)} \qquad\qquad (1.3)$$

The anisotropy parameter $(<\cos \theta>)$ is the average value of $\cos \theta$ w.r.t. differential cross section σ_θ. In case of an isotropic system, $g = 0$ *i.e.* $l_s = l^*$. For a diffusive system, we define diffusion coefficient denoted by D as

$$D = \frac{v_E l^*}{d} \qquad\qquad (1.4)$$

Here, d is the dimensionality and v_E is the energy transport velocity. Physically, l^* can be interpreted as the characteristic length before which the path of the input beam is completely randomized.
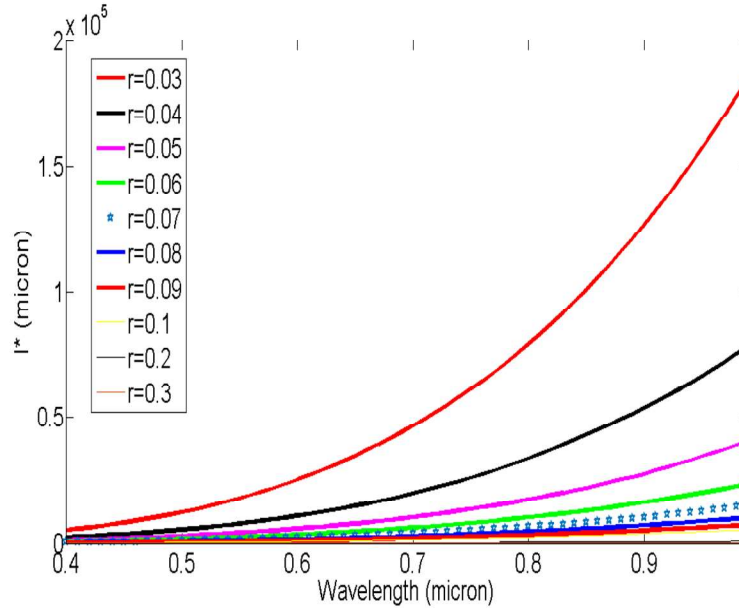
Figure 1.2: *Variation in l* for polystyrene beads with different particle size. Units of particle size: μm*

Based on input parameters like particle size, refractive index of scatterer and the surrounding medium, the Maxwell's equations are solved by Bohren-Huffman Mie theory [7] to obtain different cross-sectional area and dependent parameters such as transport mean free path (l^*) (eq. 1.3), diffusion coefficient (D) (eq. 1.4). From the Mie theory, transport mean free path (l^*) has wavelength dependence at different particle size. As seen in fig.1.2, for particle size 0.03 μm, l^* varies from 5090 μm to 1.852×10^5 μm over the wavelength range of 0.4-1 μm. This variation increases with decrease in particle size. As the transport mean free path has wavelength dependence, the response of sum of all wavelengths will be different from individual response. The response of larger wavelength range can result in variation from normal exponential decay such as stretched exponential.

In this thesis, we will be studying multiple scattering of the particles in Rayleigh range and wavelength range of 300 to 1000 nm to observe significant variation in l^* value. In order to avoid contribution from the boundaries, the thickness of the sample and the transverse sample dimensions are larger than l^*. We are studying media such as polystyrene spheres suspended in millipore water and titanium dioxide in ethylene glycol in which scattering will be prominent as particles are suspended freely. To perform the experiments, we use

two sources- supercontinuum generated from femtosecond laser source and supercontinuum generated from PCF. For a particular particle size, concentration is varied and diffusion profile is observed at one point. We have also varied the distance from the center in the transverse plane and observed the change of diffusion profile at one concentration in Fourier plane. Later on, studies could be conducted to observe the temporal behaviour of pulses when passed through the scattering media. This profile is estimated to be deviating from the exponential decay observed for single wavelength. For studying both spectral and temporal domain, understanding the input parameters for the experiment is important to make conclusions. In the next chapter, we will be concerned about the characterisation of the femtosecond laser.

Chapter 2

Femtosecond Laser as Supercontinuum Source

Supercontinuum (SC) generation is the formation of broad spectral bandwidth when high power ultra-short pulse propagates through a non-linear medium. This has high spatial coherence and low temporal coherence. The SC has a wide range of applications in optical frequency combs, nonlinear microscopy, wide-band spectroscopy, Time-Correlated Single Photon Counting (TCSPC), Flourescence Microscopy, Optical Coherence Tomography (OCT) [8, 9].

2.1   Supercontinuum Generation

SC is generated when an ultra-short pulse is passed through an optical fiber of high non-linearity. As the pulse passes through the fiber, many non-linear phenomena like dispersion of the medium, self-phase modulation, Raman scattering and phase matching and solitons causes the splitting of SC pulses into smaller pulses leading to the dispersion of pulse energy. The primary frequency of the laser to pump in the fiber is called as the primary mode. Due to the high intensity of this pulse, the refractive index of the material changes and leads of energy transfer from the primary mode to other modes. This change of refractive index when

an high-intensity pulse is passed through the medium is called as Kerr non-linearity and the transfer of energy to different modes is called as self-phase modulation. The efficiency of the SC will decide the spectral range of SC [11]. The medium chosen for SC generation can be photonic crystal fiber (PCF) or non-linear crystal like BaF_2.
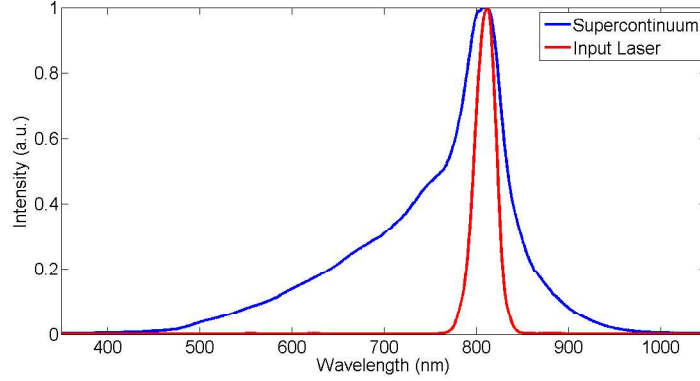

Figure 2.1: *Generation of Supercontinuum from a femtosecond laser source focused onto a BaF_2 crystal of 15mm length.*

PCF has high refractive index material like germanium doped in a silica incorporated in the cladding of lower refractive index material to allow total internal reflection in the core. The Fianium Whitelase Supercontinuum laser used for initial measurements is based on ytterbium fiber laser coupled to high index guiding PCF of the silica core and air-filled cladding [10]. The pump wavelength in this laser is 1064 nm. The laser is set up according to the non-linear effect working effectively around this wavelength by changing the core diameter and phase matching properties. Depending on the incident power of the 1064 nm, SC broadens in its proportion. The fundamental pulsewidth is 6 ps but after the generation of SC, it broadens. We need a shorter pulse laser source to probe system of the time scale smaller than picoseconds. So, we use femtosecond laser source for generation of SC. This will ensure that even if the pulse is stretched after SC generation, it will be smaller than the response of the system to be used as a probe. The femtosecond pulses at 40 mW power are passed through a non-linear BaF_2 crystal to produce SC (fig. 2.1). The pump is located around 800nm.

The generation of the ultrashort pulse is based on mode-locking technique. In general, a

laser consists of gain medium and a cavity. The cavity consists of a pair of mirrors separated by distance L with a gain medium inside it. The photon round trip in a cavity is given by T_{RT}:

$$T_{RT} = 2L/c \tag{2.1}$$

where c is the velocity of the light in the gain medium.

This round trip time (T_{RT}) determines the mode locking condition for generation of ultra-short pulse. The electric field at one of the mirrors is given by:

$$E(t) = \sum_{n=1}^{N-1} E_n sin[2\pi(\omega_o + n\delta\omega)t + \phi_n(t)] \tag{2.2}$$

where N is the number of oscillating modes, $\phi_n(t)$ is the phase of nth mode and ω_o is the lowest frequency mode above the lasing frequency. If the phase is fixed with respect to each other, *E(t)* repeats with a period of T_{RT}. One can attain this constant phase difference by active or passive mode locking. In active mode locking, an active element is placed in the laser cavity generating loss modulation synchronised with the cavity. While passive mode locking is carried out with a nonlinear device placed inside the cavity.

The femtosecond laser facility at TIFR, this mode-locked laser of 88 MHz pulse train with output power of 500mW is fed into amplifier constituting a pulse stretcher to allow more power to be fed in pulse, a pulse picker to cut the input pulse train to 1kHz, Ti:Sapphire crystal amplifier is 9-pass multi-pass amplifier in ring configuration pumped by 1kHz, Q switched Nd:YLF laser is further compressed by pulse compressor to produce femtosecond pulses of $\approx$ 40 fs with repetition rate of 1kHz [11].

Once, we understood the principle behind the femtosecond pulse generation, it is important to realize that the SC generation is highly dependent on input power, intensity and other factors. Thus, we characterise the femtosecond laser in order to get an idea of the source to be used in the subsequent experiments.

2.2   Characterisation

2.2.1   Energy Measurement

The spectral width and spectral characteristics of the SC depend on the incident pump intensity of the femtosecond laser. Therefore, this measurement is important as it gives information about the fluctuations in energy and energy is dependent on the incident intensity.
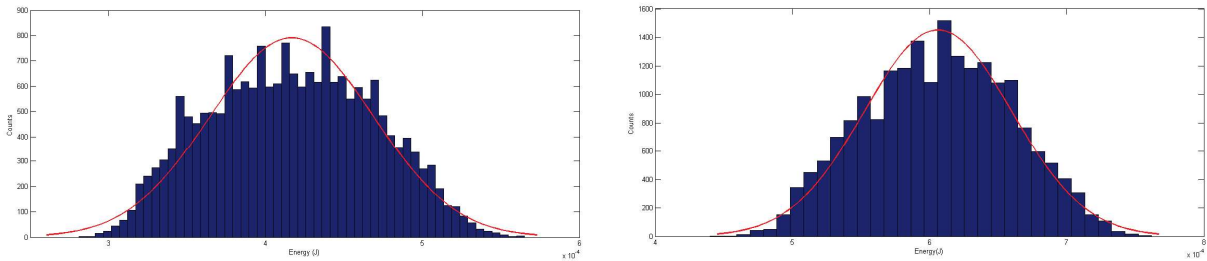

Figure 2.2: *The energy distribution of femtosecond laser for two different energy fitted with the Gaussian distribution.*

We have recorded energy of 20,000 femtosecond pulses and identified the energy with least fluctuations as 0.416×10^{-4} J and 0.606×10^{-4} J for two different input currents to the amplifier. We plan to generate our SC using these energies in future.

2.2.2   Pulse Width Measurement

The femtosecond pulse is too small to be measured by the most sensitive instruments like photomultiplier tube (PMT), photodiodes as the rise time is not smaller than 0.1 ns. Thus, autocorrelation technique, frequency resolved optical gating (FROG) and the direct electric field reconstruction (SPIDER) [12] are used for measuring ultra-short laser pulse duration. We used the autocorrelation method which involves recording the spatial profile of the second harmonic generated in a KDP crystal.

This technique is based on second-order autocorrelation measurement by splitting a laser beam into beams of equal intensity and overlapping them to produce second harmonic (SH)

[13]. The intensity of second harmonic will be proportional to the product of intensities $I(t)$ of two beams separated in time t_p.

$$A(t_p) = \int_{-\infty}^{\infty} I(t)I(t - t_p)dt \qquad (2.3)$$

By varying the time delay, t_p, the temporal profile and the width of the pulse can be directly found from the autocorrelation profile.
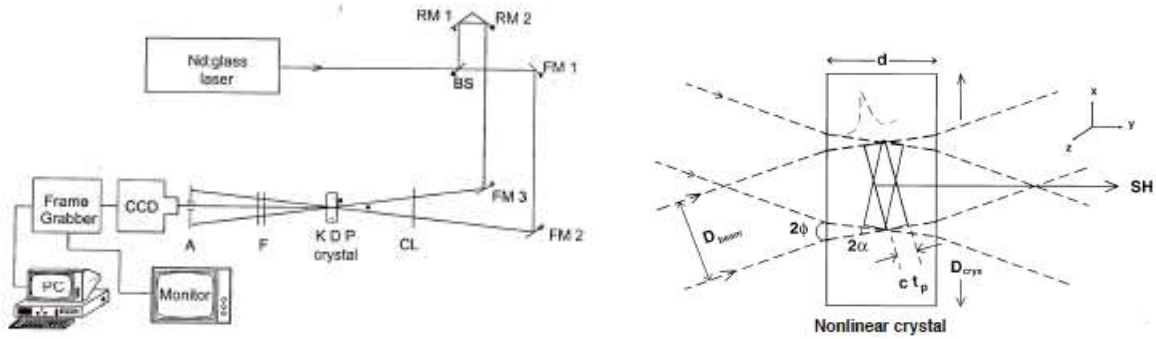

Figure 2.3: *(a) Experimental setup of single shot autocorrelator. RM: Retro mirror, FM: Folding mirror, BS: Beam splitter, CL: cylindrical lens, F: Filters, A: Apertures. (b) Schematic of single shot autocorrelator forming second harmonics along the bisector of crossover angles.*

As shown in fig 2.3 (a), the actual beam is split into two arms and made to overlap in a non-linear crystal to produce second harmonic light. If the beam waist in the overlapping area is much larger than the pulse length, ct_p, two beams overlap spatially and temporally inside the crystal. The SH signal due to overlap is directly proportional to the intensity of individual beams at each point and direction of emission is along the bisector of crossover angle. By considering phase matching condition for second harmonic, FWHM of the SH intensity profile (δx) is related to pulse duration (t_p) as :

$$\delta x = (0.77ct_p)/sin\phi \qquad (2.4)$$

This is obtained with the assumption that the pulse shape is of $sech^2$ form (only stable

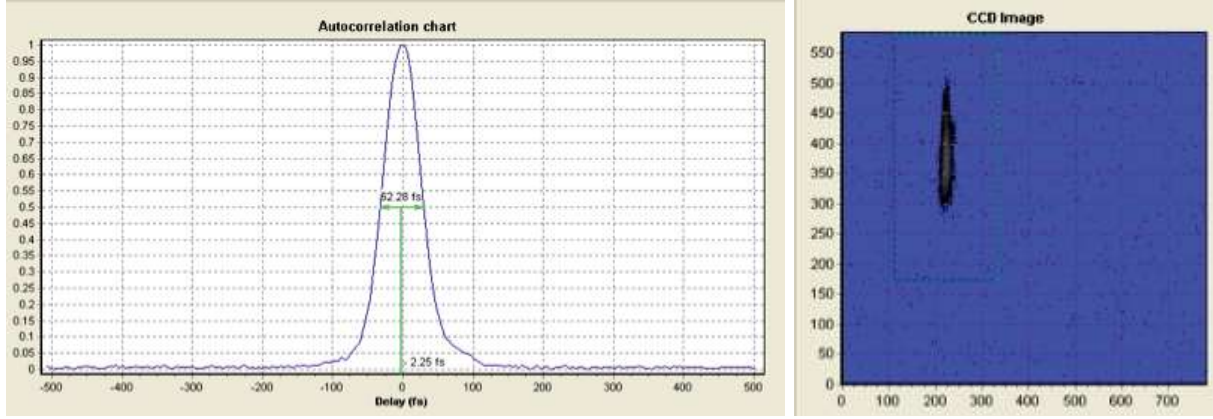solution of the evolution of pulse in a cavity). The pulse duration measured is 40.4 ±0.3 fs .

Figure 2.4: *Autocorrelation Chart and SHG Signal for the femtosecond laser beam and the pulse duration measurement by sech^2 method.*

2.2.3 M^2 Measurement

The M^2 factor is a measure for beam quality of a particular laser beam. It gives one an idea how close it is to a gaussian beam. A standard Gaussian beam which is diffraction-limited has an M^2=1. Based on this value one can find the characteristic beam width (W), Rayleigh range (Z) and beam divergence (θ), that are related as follows:

$$\theta = \frac{W_f}{f} \tag{2.5}$$

$$W = \frac{4\lambda M^2}{\pi \theta} \tag{2.6}$$

$$Z = \frac{W}{\theta} \tag{2.7}$$

where W_f is the focal length at the focus, f is the focal length of the lens. This experiment was conducted with Ophir-M^2-200-FW setup [14]. One of the challenges of measuring the

M^2 value was alignment as a slight mismatch of height and angle causes large variation in M^2 value. The pilot experiment for the same was conducted with He-Ne laser which would give Gaussian beam output with M^2 close to 1.
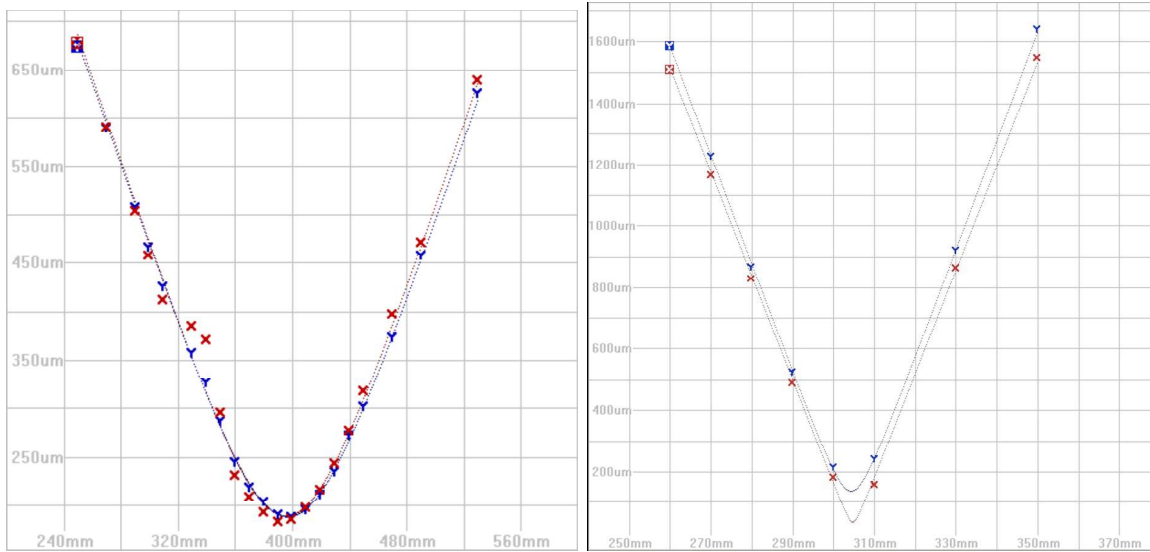

Figure 2.5: *The setup involves sweeping of the lens system near the minima of the Gaussian beam where the two axes represent the distance on X and Y axis for (a) He-Ne Laser (b) Femtosecond Laser.*

The M^2 value for He-Ne laser is 1.03-1.07 (fig. 2.5 (a)) which agrees with Gaussian beam . Same experiment when done for femtosecond laser (fig. 2.5 (b)), a discrepancy was observed in M^2 value of X (1.197) and Y (4.810) axis .This discrepancy is within the femtosecond laser system.

In conclusion, we have characterised the femtosecond laser used for the experiments.

Chapter 3

Imaging through random media

The study of wave propagation through a random media is of prime importance in the fields of biomedical imaging [15], colloidal optics, astronomy, acoustics [16]. In the field of biomedical imaging, it has played a key role in determining the size, shape and location of the foreign object inside a tissue . Analogous to such a system, studying propagation of light through random media will help to understand the nature of the scatterer.

3.1   Ballistic, Snake and Diffuse photons

When light is passed through a random media, it has three types of outgoing photons i.e. ballistic, snake and diffuse photons.

The photons undergoing least number of scattering events without any loss of coherence is ballistic. They tend to be in the same direction as the propagation direction. But the multiply scattered light undergoes large number of scattering events leading to deviation from the forward direction. These diffuse photons lose the coherence as the path has been completely randomised due to multiple scattering in the medium. Apart from ballistic and diffuse photons, photons experiencing collision with the scatterers which changes the angle of propagation but still wander close to the propagation axis are defined as "snake" photons. This motion is analogous to movement of snake.

As shown below, red line represents ballistic photons, orange color denotes snake photons and blue path is the path taken by diffuse photons. As the number of scattering events is an important feature for determination of the type of photons, it becomes obvious that the first photons to exit from the scattering medium will be one with minimum number of scattering events i.e. ballistic photons and diffuse photons are the last.
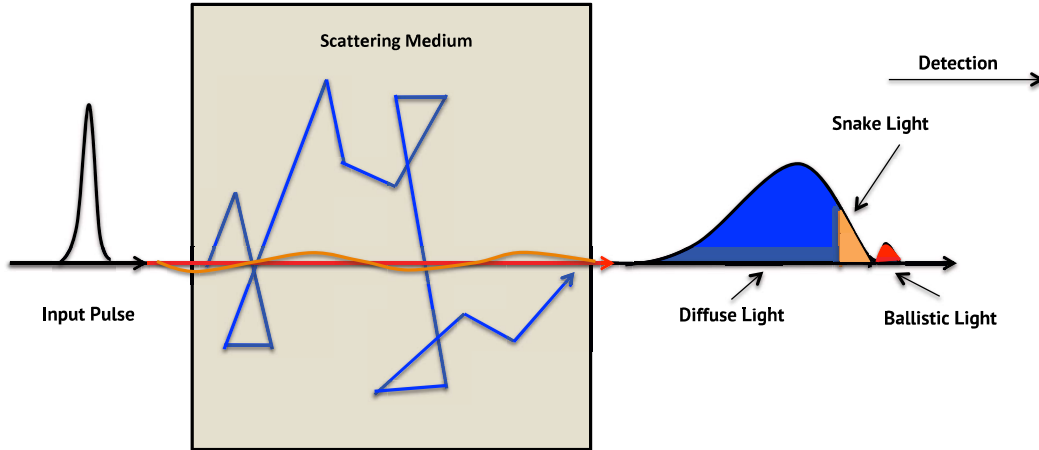

Figure 3.1: *The type of photons viz. ballistic, snake and diffuse photons and time at which they exit the sample.*

The separation of ballistic and diffuse photons is possible both spatially and temporally. Throughout this thesis, ballistic and diffused light will be studied but more focus will be given on the study of diffused light in diffusion approximation.

3.2 Scattering Media

Our focus is on studying diffusive systems. For designing the sample, we need a sample with large contrast of refractive index to have measurable diffusion effects. Thus, we use polystyrene spheres (0.3± 10%) μm in millipore water which has refractive index contrast-1.19 (refractive index of polystyrene spheres: 1.59 , refractive index of millipore water: 1.33). This has been widely studied for scattering experiments and they remain suspended for a
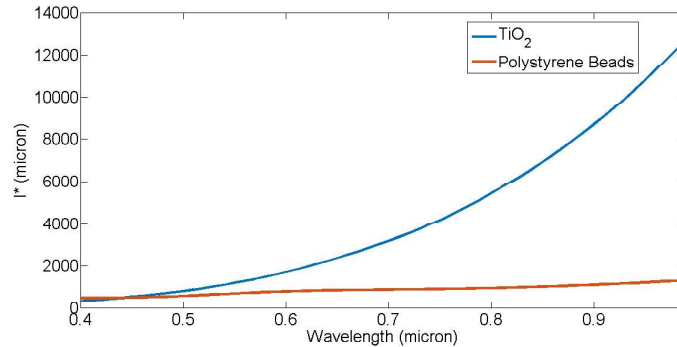
long time which has an added advantage.

Figure 3.2: *The l* value of TiO₂ in ethylene glycol and polystyrene suspended in millipore water has a large variation in the value for a given wavelength range for comparable number density per unit volume (N) and the chosen particle size for the experiment.*
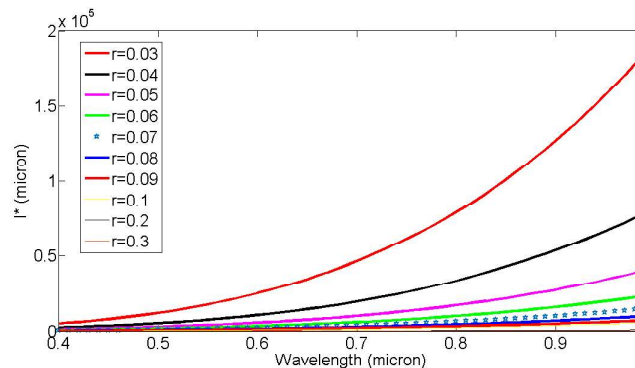

Figure 3.3: *Smaller particle size provides advantage of larger variation in l* as the percentage change in l* is large.*

As shown in fig. 3.2, larger variation in the l^* is observed for TiO₂ suspended in ethylene glycol where refractive index contrast is 1.82 .Thus, choosing it over polystyrene offers an advantage while studying the collective response of the system. Another reason for this large variation is the smaller particle size of TiO₂ as small particle size has more variation in l^* in the wavelength range from 400 to 1000 nm (fig. 3.3). As shown in the fig. 3.4, average particle size is estimated to be 35 nm.It has agglomeration and settling issues but we have tried to eliminate it by continuous stirring of the scattering media for consistent study.
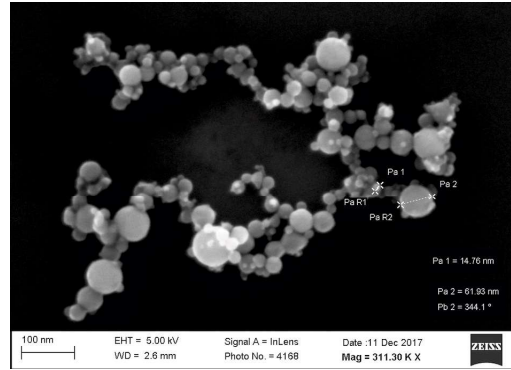
Figure 3.4: *SEM Images of titanium dioxide suspended in ethylene glycol for estimation of particle size.*

For both the cases, we have found out concentrations in the range where prominent spectral variation can be observed. For polystyrene, we chose the master solution of $N=0.71 \times 10^{13}$ /cc (VF=0.1). This has been further diluted to $N=1.77 \times 10^{10}/cc$ (VF=0.00025). While, for TiO$_2$, $N= 1.06 \times 10^{16}/cc$ (VF=0.24) diluted to $N= 1.73 \times 10^{15}/cc$ (VF= 0.038) as master solution and concentration is varied around these concentrations.

3.3   Spectral Response

3.3.1   Experimental Setup for pilot experiment

For the initial measurements, pilot experiments were conducted with Fianium WhiteLaser supercontinuum laser. This laser offers broad spectral range with the pump at 1064 nm and passed through PCF to obtain ultra-broadband range of 400-1000 nm. This laser is collimated using a small lens placed quite close to the source. This 1 cm spot size beam is passed through the medium placed in glass cuvette of dimensions 5×5×2 cm. We have particularly chosen the sample thickness to be larger than l^* to observe diffusion phenomenon.
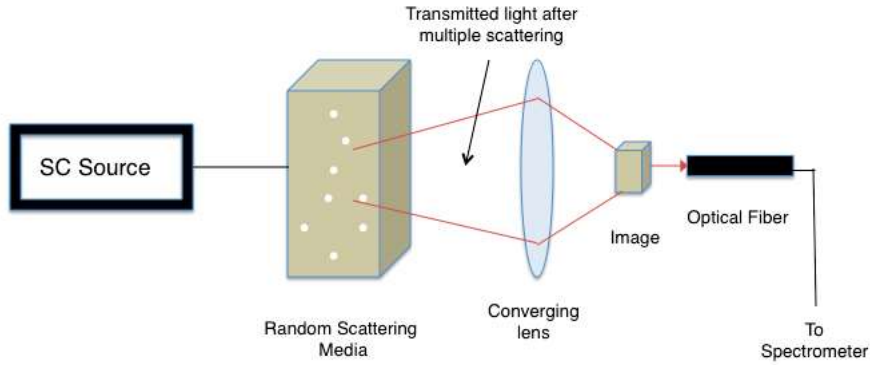
Figure 3.5: *Schematic of the experimental setup with random media as 0.3 μm of polystyrene suspended in millipore water and converging lens to reduce the area which is scanned by optical fiber connected to the spectrometer.*

We collect the forward scattered light through series of lens with variable *f*. This image plane is imaged with a multi-mode fiber of 400 μm core diameter. The size of the image in the image plane is 5×5 mm. The spectra was collected from wavelength 400 to 1000nm at different points in the image plane.

Results

Image Plane

As a source, Fianium Whitelase supercontinuum laser with 100-500mW input power is used. We measure spectra of ballistic photons and observe the behaviour at varying concentration. As shown in the fig. 3.6., not much variation in the spectrum is observed. This possible discrepancy is due to presence of multiply scattered photons along with the ballistic photons. However, if we do measurements off-axis, the main contribution will be from multiply scattered photons.

At a point away from axis (fig. 3.7 (a), (b)), we observe the shift of the spectrum towards higher wavelengths as the concentration increases. As N increases, smaller wavelengths will tend to diffuse faster due to smaller l^* value than longer wavelengths. This is supported by the fact the l^* value signifies the length after which the path randomises and enters diffusion regime. As a whole, the transmitted light will have less contribution from smaller
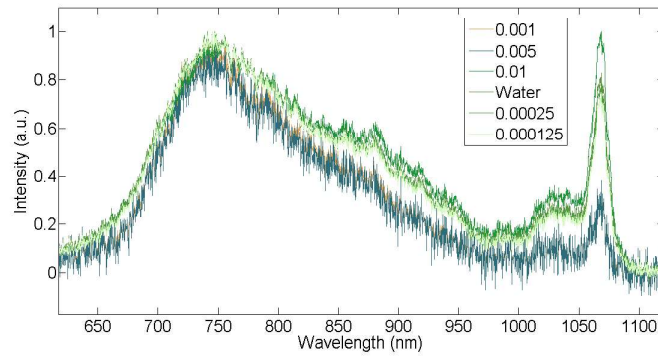
Figure 3.6: *Ballistic Beam Transmission through polystyrene beads suspended in millipore water without any large variation in the spectral characteristics.*
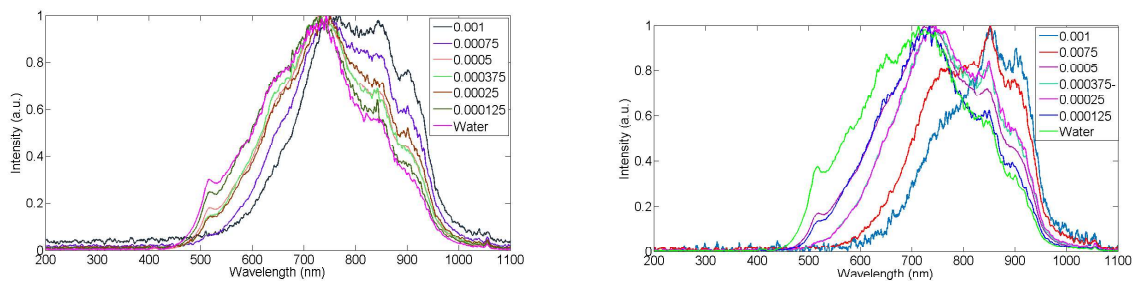

Figure 3.7: *Diffused Beam Transmission through polystyrene beads suspended in millipore water at varying volume fraction. (a) For smaller cuvette length - 1 cm (b) For larger cuvette length - 2 cm for the same volume fraction of polystyrene beads suspended in millipore water.*

wavelengths as it has been diffused and large contribution from larger wavelength light as it has not been diffused much. When normalized, the peak shift towards larger wavelengths *i.e.* blue shift observed due to suppression of smaller wavelengths by diffusion. This effect becomes prominent when the number of scattering events is increased. For example by increasing the sample length (Refer fig. 3.7 (a)- sample length is 1cm, (b)- sample length is 2 cm).

Here, we observe red shift and blue shift with the variation in concentration. In the study conducted, we conclude that we need large length of the cuvette to observe the diffusion with large variation of l^*. So, it is better to perform experiments with TiO_2 with large cuvette length and small particle size than used for polystyrene balls. Similar method is employed to perform experiments with femtosecond laser source.

Fourier Plane

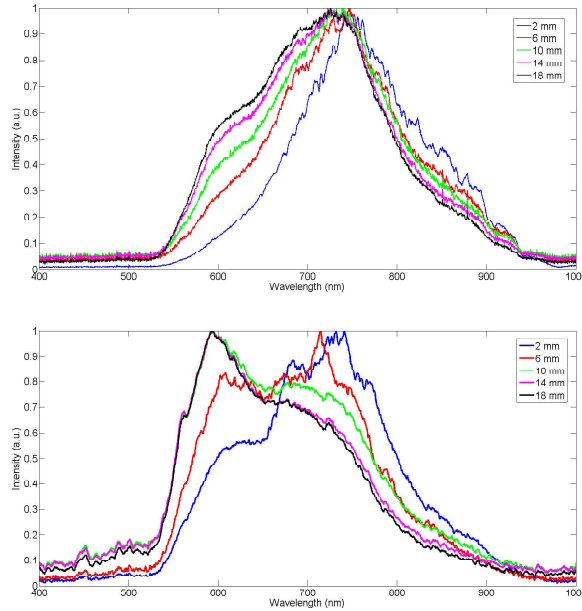We perform the similar experiment in Fourier plane to separate wave vectors $(\vec{k})$.

Figure 3.8: *Change in spectra in Fourier plane at varying distances from the center for VF=0.00075 (up), VF=0.000125 (down) of polystyrene beads in millipore water. The change in the spectra towards smaller wavelengths at larger distances shows diffusion to be prominent at larger distances from the center.*

In fig. 3.8, close to the propagation axis (at 2 mm distance from the center), we observe smaller $\vec{k}$ vectors *i.e* less diffuse photons contribute to the measurement. For larger distances (at 18 mm distance from the center), $\vec{k}$ varies largely from the input $\vec{k}$ which implies that it has undergone multiple scattering events. In fig. 3.8, for VF=0.00075, there is no change in spectrum with change in distance from the center implying that diffusion is not prominent. At VF= 0.000125, we can clearly see in fig. 3.8, lower wavelengths contribute more at larger distances. This indicates that we observe more diffusion towards the edges than at the center.

3.3.2   Experimental Setup

For the spectral measurement, 1kHz femtosecond laser is operated at 1mJ. The beam of spot size 1 cm was focused on a cylindrical 15mm long non-linear Barium Fluoride (BaF_2) crystal using lens of f=10cm to generate SC [11]. The beam is collimated and is incident on the glass cuvette of dimensions 5×5×2 cm used as sample holder. The glass cuvette contains scattering media *i.e.* TiO_2 in ethylene glycol. The scattered light is collected using 3-inch lens of f=8.5cm and spectra is recorded by fiber coupled spectrometer (Ocean Optics USB4000).
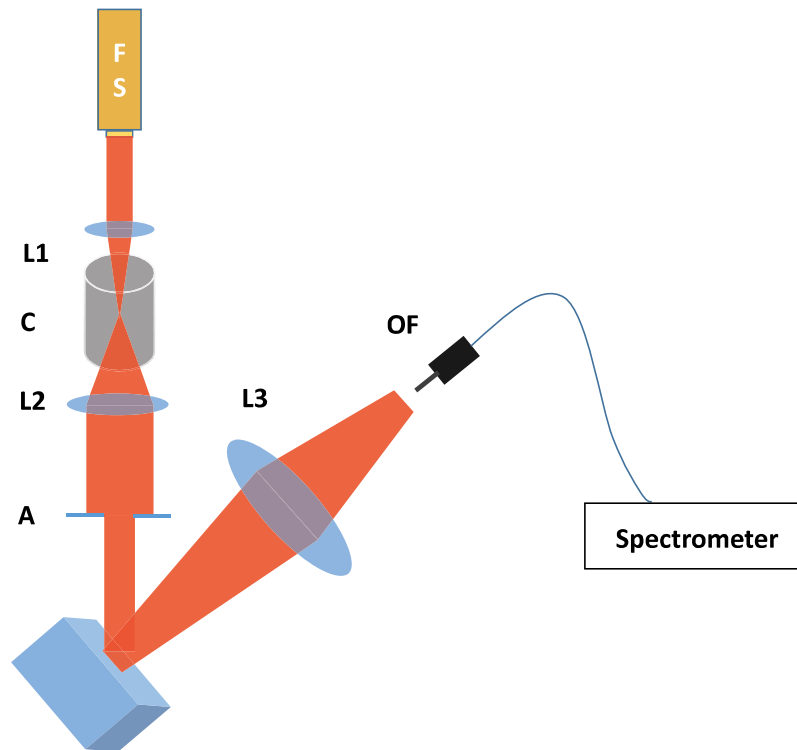
Figure 3.9: *Schematic of the experimental setup for the backscattering performed with Femtosecond Laser when focused onto BaF$_2$ crystal which generates supercontinuum incident on the TiO$_2$ suspended in ethylene glycol (scattering media) and the backscattered light is collected by optical fiber which can collect the maximum backscattered light.*
FS-Femtosecond Laser, L1,L2,L3- Lens, C- BaF$_2$ crystal, A- Aperture, OF-Optical Fiber

Results

The TiO$_2$ sample being highly concentrated doesn't allow transmission through the sample. Instead we choose to look at the backscattered light as the information about the diffused light is same for forward scattering and backward scattering. [5] [6]
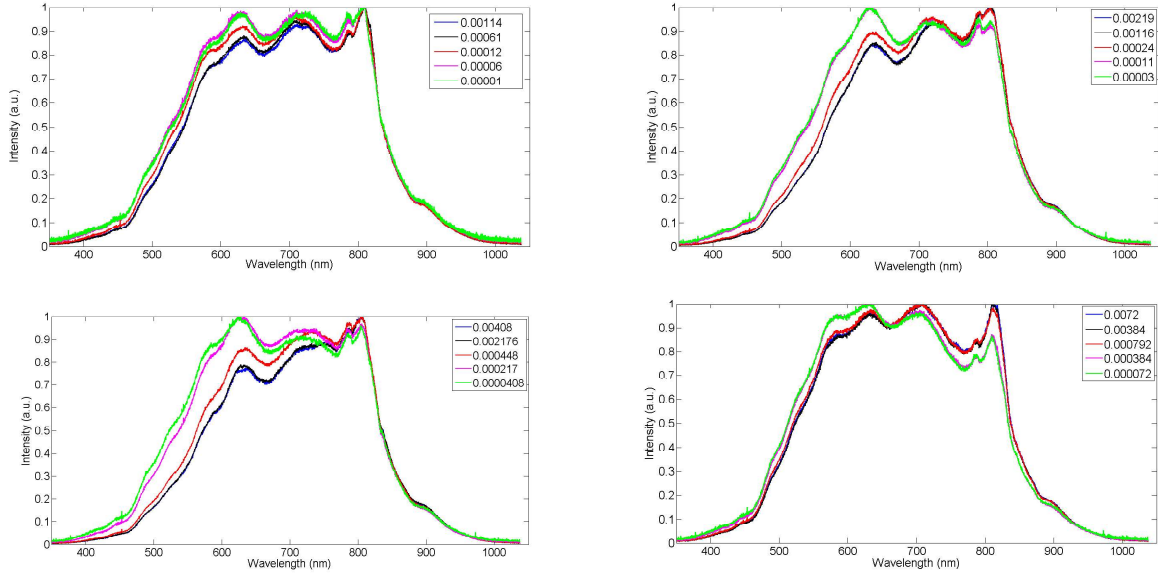
Figure 3.10: *The spectra for variable VF changed for two orders of magnitude. The largest shift in spectra is observed in the range of VF= 0.00408 to 0.0000408*

For diffusion to be spectrally observed, we need large spectral variation with concentration and we employ trial and error method to find out the concentration range suitable for temporal measurement. We increase the concentration and observe if any visible variation in spectrum is obtained in backscattered direction.These measurements are done by collecting maximum backscattered light focusing on the optical fiber. When the concentration is increased, we observe suppression of lower wavelengths than larger wavelength as expected. Amongst the concentration chosen, working in the range of VF= 0.00408 to 0.0000408 is suitable to observe the shift. We are concerned about this shift (fig. 3.10) in the spectrum towards lower wavelengths when the concentration increases as it depicts the variation of l^*. As l^* signifies the decay of each wavelength in the temporal domain and large variation in l^* will help to identify the collective behaviour of ultra-broadband light.

3.4 Temporal Response

3.4.1 Theory

For the quantitative analysis of the multiply scattering events, we first solve the diffusion equation suitable for our system and look at its behaviour for different types of photons in temporal domain. Within the diffusion approximation, the intensity distribution $(I(r,t))$ is governed by the second order differential equation: [19]

$$\frac{\partial I(r,t)}{\partial t} = D\nabla^2 I(r,t) - \frac{v}{l_i} I(r,t) + S(r,t) \qquad (3.1)$$

where v is the energy transport velocity, l_i is the absorption length (wavelength dependent) and $S(r,t)$ is the source term. The temporal point spread function of the transmitted light is predicted by the diffusion equation is [17]:

$$I_{tr}(t) = \frac{D}{\pi L^2} \sum_{n=1}^{\infty} n \left(\frac{\pi L}{L_{eff}}\right)^2 sin\left(\frac{n\pi L}{L_{eff}}\right) \times exp\left[-Dt\left(\frac{n\pi}{L_{eff}}\right)\right] exp\left(\frac{-vt}{l_i}\right) \qquad (3.2)$$

where $L_{eff} = L + 2z_0$, where L is the system size. The parameter $z_0 = 0.71 \times l^*$ is the extrapolation length, l^* being the transport mean free path. For more details on this solution, refer [17] This model is true only in the limit when the thickness of the sample is minimum one order larger than the transport mean free path. (Thickness $> 13 \times l^*$) [18]. In the sample chosen, we have variation of l^* from 147 μm for 600 nm to 4 cm for 1000 nm wavelength (Polystyrene balls). For TiO_2, we calculate that l^* varies from 300 μm for 600 nm to 5 cm for 1000 nm wavelength. From these values, the system is assumed to be in diffusion regime as kl^* value is much larger than 1. As it can be seen, l^* itself is larger than the thickness of the sample for larger wavelength like at 1000 nm. The SC intensity at this wavelength is very small (Refer fig. 2.1) so we can assume this model to be valid. Moreover, the larger wavelengths won't be contributing to the decay of the sample and will be a part of the ballistic component itself. In the long time limit, in absence of absorption and source term i.e. $S(r,t)=0$ and $v = 0$, the exponential decay has time constant (τ) :

$$\tau = \frac{(L + 2z_o)^2}{D\pi^2} \qquad (3.3)$$

3.4.2   Numerical Calculation

The behaviour of ultrashort pulse after passing through disordered media is studied in frequency domain. In the calculation, we considered the disordered random medium to be of 0.3μm polystyrene beads suspended in millipore water in a rectangular slab. The intensity distribution of the source is neglected and temporal profile is calculated using eq. 3.2.
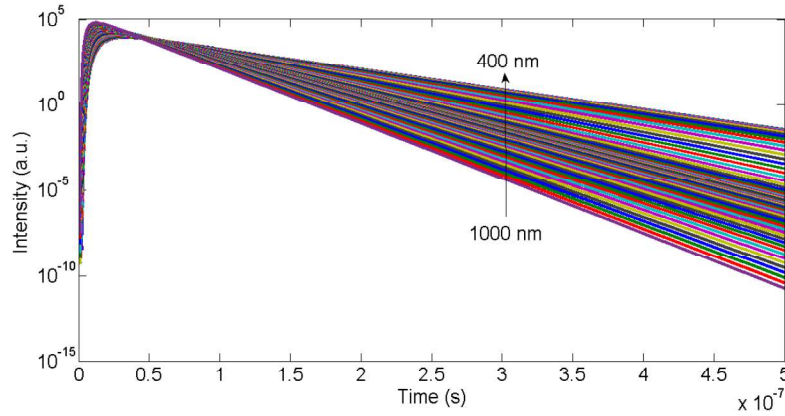

Figure 3.11: *Temporal profile of individual of wavelength range from 400 to 1000 nm for polystyrene beads suspended in millipore water with N= 7.07 $\times$ 10^{12}/cc*

We know that for a 'single wavelength' pulse undergoes an exponential decay. In this case, the decay depends on the *l** value and can be fitted with an exponential given as:

$$I \propto exp(-t/\tau) \qquad (3.4)$$

The τ value is chosen as a function of wavelength. Therefore, τ is faster for larger wavelengths than shorter wavelength. For a broadband source, the decay is a sum of eq. 3.4 for different wavelengths (different τ value) will be a stretched exponential decay. Looking at the temporal distribution from t=0 (fig. 3.12), we see ballistic part reaching the earliest. The diffuse photons which show the stretched exponential behaviour reach later. The diffused part of the beam for a single wavelength is decaying exponentially as seen in fig.2.6.
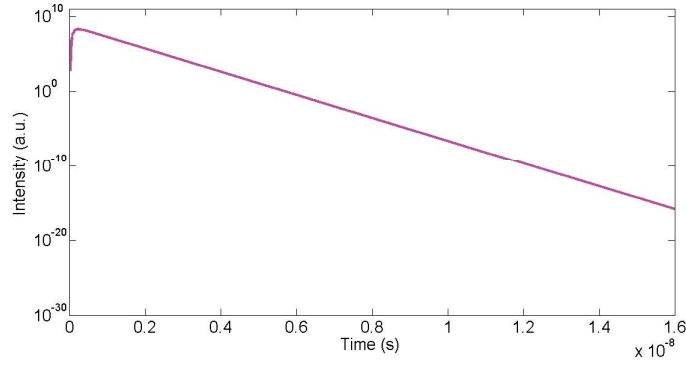
Figure 3.12: *Temporal distribution with ballistic, quasi-ballistic and diffuse photons in semilog scale.*

If the similar distribution (fig.3.11) is obtained for titanium dioxide in ethylene glycol, we observe that for the same wavelength range there is a large variation in the decay times for different wavelengths (fig.3.13). This is a result of the small particle size of TiO_2 and large refractive index contrast in the solution.
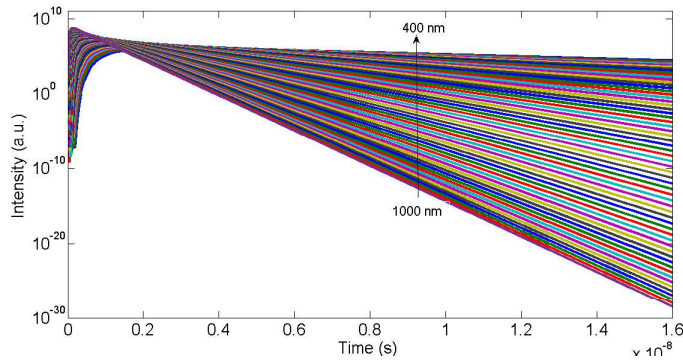

Figure 3.13: *Temporal distribution for individual wavelength for TiO_2 suspended in ethylene glycol with N=4.4544 $\times$ 10^{14}/cc.*

The individual wavelengths have exponential decay with τ value dependent on the wavelength, the resultant behaviour of all wavelengths in diffusive region is a generalised stretched exponential decay given by :

$$I \propto exp(-t/\tau)^{\beta} \qquad (3.5)$$

where β is the stretching exponent.

The stretched exponential is prominent when we have large variation of τ of individual wavelength. Thus, we see in fig. 3.14 and fig. 3.15, for polystyrene and TiO_2, the sum of all wavelengths will be a stretched exponential decay in diffusive region.
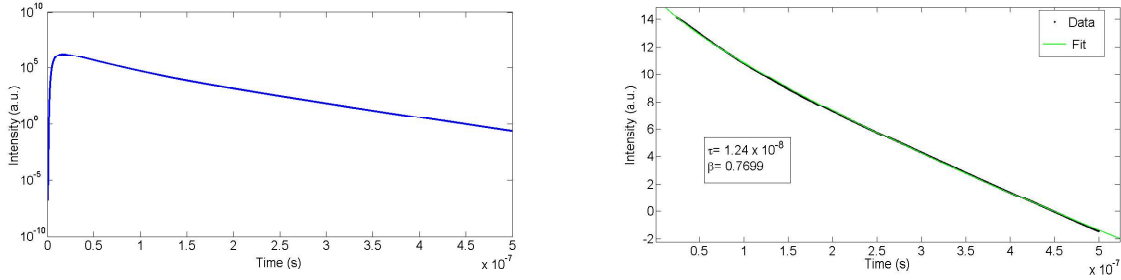

Figure 3.14: *Sum of all wavelengths in fig 3.10 results in stretched exponential for polystyrene beads- different from normal exponential for single wavelength as seen in fig 3.11. It has been fitted to obtain stretched exponential parameters.*
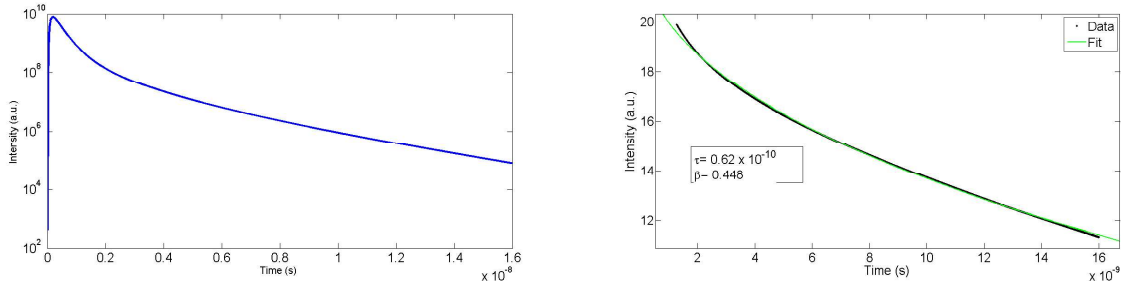

Figure 3.15: *Sum of all wavelengths is a stretched exponential for TiO_2 is summed from 400 to 1000 nm and fitted with stretched exponential equation.*

In the diffusion region, we fit eq. 3.5 and obtain $\tau = 1.24 \times 10^{-8}$ and $\beta = 0.7699$ for polystyrene which shows stretched exponential behaviour. But larger stretched exponent decay is clearly visible for TiO_2 as $\beta = 0.448$ which signifies large shift from normal exponent curve.

Now that we have identified the time scales, we want to measure the decay to obtain parameters *viz.* τ and β. Experimentally, this can be achieved by doing time domain measurements using very sensitive ultrafast detectors or streak camera.

We looked at the decay using ALPHALAS ultrafast detector - UPD-30-VSG-P has spectral range of 320-900 nm with rise time less than 30 ps. As seen from the numerical simulations, the τ is of the order larger than 1000 ps. Thus, it should be resolved with this ultrafast detector.
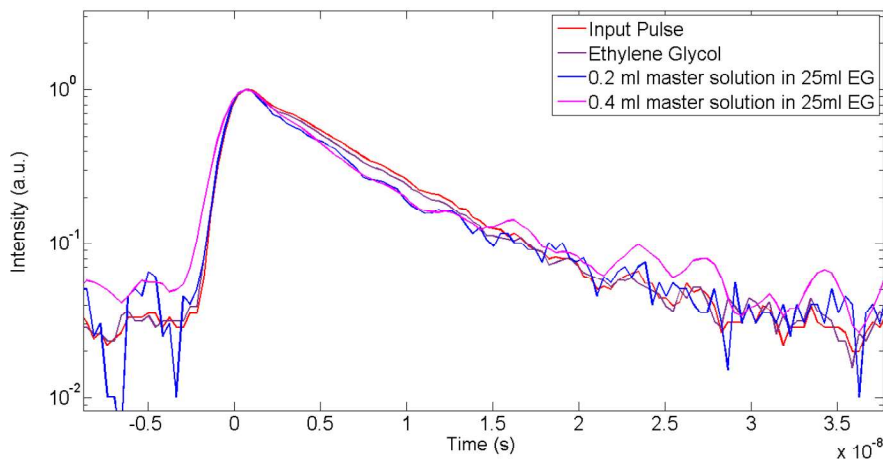

Figure 3.16: *The response of the detector along with the decay of the scattering media for variable concentration. Master Solution : N=2.2046 $\times$ 10^{14} /cc*

As seen above, the fluctuations in the sample itself was large enough that the exponential tail couldn't be resolved. Moreover, the response of the detector itself was extending to few nanosecond that resolving the exponential decay of the sample excluding the decay of the detector is difficult. Thus, we switch to more sophisticated instrument to do time domain measurements.

Chapter 4

Conclusion and Further Outlook

The spectral measurement from randomly scattered media provides information about the particle size, transport mean free path and characteristics essential for biomedical imaging. Along with the application, there is a lot of physics involved in the process of understanding the behaviour of such systems.

In evaluation of this study, the femtosecond laser for supercontinuum generation was well characterised for the beam width, M^2 value and pulse width. The scattering media *viz.* polystyrene beads in millipore water and TiO_2 in ethylene glycol are well studied for diffusion. We have identified the advantages of working with TiO_2 than polystyrene beads. It offers better contrast in refractive index and smaller particle size leads to smaller transport mean free path (l^*) and larger variation of l^* for the wavelength range of 400-1000 nm under study. With increase in concentration, for diffused light, we observed the redshift of wavelengths signifying that smaller wavelengths scatter more than larger wavelength which clearly agrees with eq.1.1 and fig.3.3. While for ballistic light, no variation was observed which agrees with the property of ballistic light (fig.3.6). The scan for spectrum was done in image plane and fourier plane. In image plane, we observe shift of spectra towards smaller wavelengths with decrease in concentration (fig.3.7). In Fourier plane, we measure the spectra at different distances from the center and observe that for smaller concentration prominent diffusion is seen at the periphery (fig.3.8).

Clear indication of properties of ballistic and diffuse photons are stated and studies focused on diffused light are mainly performed. The stretched exponent behaviour is observed

31

in forward direction. For the time domain, model is chosen without assuming absorption in the system. The decay of the wavelength 400-1000 nm is calculated individually which is an exponential decay and collectively is a stretched exponent (fig.3.12, fig.3.14). The β parameter defines the stretched parameter and deviation from normal exponent (fig 3.15) which is observed for single wavelength (fig. 3.13). The resultant τ and β is estimated from the stretched exponential fit. This calculated decay time can be further compared with the value obtained by measuring the decay time with ultrafast detector or streak camera.

We use ultrafast ALPHALAS detector with rise time less than 30 ps to measure decay of the pulse through the random media. The response of the detector interferes with the signal. Normal tests like measurement of nanosecond pulse was identified but resolving picosecond pulse was difficult.The problem can be resolved by performing experiments on streak camera. Initial test of measurements of stretched exponential for green pulsed picosecond and nanosecond laser are observed but for the SC from femtosecond laser this is yet to be seen. These measurements are to be performed to understand the collective nature of the ultra-broadband pulse passing through a diffusive system.

This project is open for new questions like resolving the signal by ultrafast detector and understanding the features of the response of system in time domain and the resultant τ value. This can be addressed by streak camera which provides large spectral range of 230-950 nm with sensitivity upto 2 ps. Future experiments will be focused on estimating l^* experimentally with streak camera for individual wavelength.

In conclusion, this project has opened large number of questions to understand the temporal domain of diffused systems and experiments further associated with the same.

Bibliography

[1] P. W. Anderson,*"Absence of Diffusion in Certain Random Lattices"*, Phys. Rev. 109, 1492 (1958).

[2] J. Binding, J. Ben Arous, J. F. Leger, S. Gigan, A. C. Boccara, L. Bourdieu, *"Brain refractive index measured in vivo with high-NA defocus-corrected full-field OCT and consequences for two-photon microscopy"*, Optics Express 19, 4833 (2011).

[3] Diego Di Battista, Giannis Zacharakis and Marco Leonetti, *"Enhanced adaptive focusing through semi-transparent media"*, Scientific Reports 5, 17406 (2015).

[4] James R. Nagel and Michael A. Scarpulla, *"Enhanced absorption in optically thin solar cells by scattering from embedded dielectric nanoparticles"*, Optics Express 18, A139 (2010).

[5] Michael S. Patterson, B. Chance, and B. C. Wilson, *"Time resolved reflectance and transmittance for the noninvasive measurement of tissue optical properties"*, Appl. Opt. 28, 2331-2336 (1989)

[6] Delpy, David T., Mark Cope, Pieter van der Zee, S. R. Arridge, Susan Wray, and J. S. Wyatt. *"Estimation of optical pathlength through tissue from direct time of flight measurement."*, Physics in Medicine & Biology 33, no. 12 (1988): 1433.

[7] *"Rayleigh & Mie scattering cross section calculations and implications for weather radar observations"*- http://www.ou.edu/radar/module01radarApps.pdf

[8] C.F. Kaminski, R.S. Watt, A.D. Elder, J.H. Frank, J. Hult, *"Supercontinuum radiation for applications in chemical sensing and microscopy"*, Appl. Phys. B (2008) 92: 367

[9] Norihiko Nishizawa, *"Generation and application of high-quality supercontinuum sources"*, Optical Fiber Technology, Volume 18, Issue 5, Pages 394-402 (Sept 2012)

[10] *"Supercontinuum Generation in Photonics Crystal Fibers- Thorlabs"*, V2.0 (July 2009)

[11] A. K. Dharmadhikari, F. A. Rajgara, N. C. S. Reddy, A. S. Sandhu, and D. Mathur, *"Highly efficient white light generation from barium fluoride"*

[12] Matthias Wollenhaupt , Andreas Assion , Thomas Baumert, *"Femtosecond Laser Pulses: Linear Properties, Manipulation, Generation and Measurement"*, Springer Handbook of Lasers and Optics, pp 937-983 (2007)

[13] M. Raghuramaiah, AK Sharma, PA Naik, PD Gupta, RA Ganeev, *"A second-order autocorrelator for single-shot measurement of femtosecond laser pulse durations"*, Sadhana, pp 603-611, (2011)

[14] *M2-200/200s-FW Users Guide - Beam Propagation Analyzer*

[15] O. Katz, P. Heidmann, M. Fink, S. Gigan, *"Non-invasive real-time imaging through scattering layers and around corners via speckle correlations"*, Nature Photonics 8, 784 (2014).

[16] S. Chandrasekhar, *"Radiative Transfer"*, Dover Publications, Inc., New York (1960).

[17] Melvin Lax, V. Narayanamurti, R.C. Fulton, *"Classical Diffusion Photon Transport in a Slab"* in J.L. Birman, H.Z. Cummins, A.A. Kaplyanskii (Eds.), Proceedings of the Symposium on Laser Optics of Condensed Matter, Leningrad, June 1987, Plenum, New York, (1987) p. 229.

[18] Z. Q. Zhang, I. P. Jones, H. P. Schriemer, J. H. Page, D. A. Weitz, and Ping Sheng *"Wave transport in random media: The ballistic to diffusive transition"*, Phys. Rev. E 60, 4843 (1999).

[19] Mujumdar, S and Dice, GD and Elezzabi AY, *"Few-cycle pulse propagation in multiple scattering media"*, Optics communications (2005)